



# Carbonic anhydrases CA1 and CA4 function in atmospheric CO<sub>2</sub>-modulated disease resistance

Yeling Zhou<sup>1</sup> · Irene A. Vroegop-Vos<sup>1</sup> · Anja J. H. Van Dijken<sup>1</sup> · Dieuwertje Van der Does<sup>2</sup> · Cyril Zipfel<sup>2,3</sup> · Corné M. J. Pieterse<sup>1</sup> · Saskia C. M. Van Wees<sup>1</sup>

Received: 5 October 2019 / Accepted: 25 February 2020  
© The Author(s) 2020

## Abstract

**Main conclusion** Carbonic anhydrases CA1 and CA4 attenuate plant immunity and can contribute to altered disease resistance levels in response to changing atmospheric CO<sub>2</sub> conditions.

**Abstract** β-Carbonic anhydrases (CAs) play an important role in CO<sub>2</sub> metabolism and plant development, but have also been implicated in plant immunity. Here we show that the bacterial pathogen *Pseudomonas syringae* and application of the microbe-associated molecular pattern (MAMP) flg22 repress CA1 and CA4 gene expression in *Arabidopsis thaliana*. Using the CA double-mutant *calca4*, we provide evidence that CA1 and CA4 play an attenuating role in pathogen- and flg22-triggered immune responses. In line with this, *calca4* plants exhibited enhanced resistance against *P. syringae*, which was accompanied by an increased expression of the defense-related genes *FRK1* and *ICS1*. Under low atmospheric CO<sub>2</sub> conditions (150 ppm), when CA activity is typically low, the levels of CA1 transcription and resistance to *P. syringae* in wild-type Col-0 were similar to those observed in *calca4*. However, under ambient (400 ppm) and elevated (800 ppm) atmospheric CO<sub>2</sub> conditions, CA1 transcription was enhanced and resistance to *P. syringae* reduced. Together, these results suggest that CA1 and CA4 attenuate plant immunity and that differential CA gene expression in response to changing atmospheric CO<sub>2</sub> conditions contribute to altered disease resistance levels.

**Keywords** Arabidopsis · CO<sub>2</sub> metabolism · Defense signaling · Plant immunity · *Pseudomonas syringae*

## Abbreviations

CA Carbonic anhydrase  
ET Ethylene  
JA Jasmonic acid

MAMP Microbe-associated molecular pattern  
*Pst* *Pseudomonas syringae* pv. *tomato* DC3000  
*Psm* *Pseudomonas syringae* pv. *maculicola* 4326  
PTI Pattern-triggered immunity  
SA Salicylic acid

**Electronic supplementary material** The online version of this article (<https://doi.org/10.1007/s00425-020-03370-w>) contains supplementary material, which is available to authorized users.

✉ Saskia C. M. Van Wees  
s.vanwees@uu.nl

Yeling Zhou  
zhouyl@sustech.edu.cn

Irene A. Vroegop-Vos  
i.vroegop@sglssystem.com

Anja J. H. Van Dijken  
a.j.h.vandijken@uu.nl

Dieuwertje Van der Does  
dieuwertje.van-der-does@jic.ac.uk

Cyril Zipfel  
cyril.zipfel@tsl.ac.uk

Corné M. J. Pieterse  
c.m.j.pieterse@uu.nl

<sup>1</sup> Plant-Microbe Interactions, Department of Biology, Science4Life, Utrecht University, Padualaan 8, 3584 CH Utrecht, the Netherlands

<sup>2</sup> The Sainsbury Laboratory, University of East Anglia, Norwich Research Park, Norwich NR4 7UH, UK

<sup>3</sup> Department of Plant and Microbial Biology, Zürich-Basel Plant Science Center, University of Zürich, Zurich, Switzerland

## Introduction

Plants have evolved a complex immune system to regulate survival from attack by pathogenic microbes and herbivorous insects. Upon perception of microbe-associated molecular patterns (MAMPs) by pattern recognition receptors (PRRs), defense responses are activated, including stomatal closure, production of reactive oxygen species, MAP kinase activation, hormonal signaling, and massive transcriptional reprogramming, which leads to the production of defensive compounds that limit pathogen ingress (Tsuda and Katagiri 2010; Zipfel and Robatzek 2010; Couto and Zipfel 2016). These induced signal outputs collectively lead to pattern-triggered immunity (PTI), which forms the first layer of plant defense to invading microbes. Evidence is accumulating that changing climate conditions can have profound effects on plant resistance pathways (Noctor and Mhamdi 2017; Kazan 2018; Velasquez et al. 2018). Atmospheric CO<sub>2</sub> is an important parameter of climate change. Changes in atmospheric CO<sub>2</sub> levels can affect disease development in diverse plant-pathogen interactions (Chakraborty et al. 2000; Garrett et al. 2006; Zavala et al. 2013; Mhamdi and Noctor 2016; Zhou et al. 2017; Williams et al. 2018b). Elevated CO<sub>2</sub> caused reduced multiplication of *potato virus Y* in tobacco plants (Matros et al. 2006) and decreased downy mildew severity in soybean plants (Eastburn et al. 2010). In contrast, the susceptibility of wheat plants to *Fusarium pseudograminearum* was increased by elevated CO<sub>2</sub> (Melloy et al. 2014). In tomato, elevated CO<sub>2</sub> levels rendered the plants more resistant to *Pseudomonas syringae* pv. *tomato* DC3000 (*Pst*), while the level of resistance against *Botrytis cinerea* decreased (Zhang et al. 2015). Furthermore, exposure of the model plant species *Arabidopsis thaliana* (hereafter *Arabidopsis*) to pre-industrial, current and future levels of atmospheric CO<sub>2</sub> uncovered marked effects on plant immunity against diverse (hemi) biotrophic and necrotrophic pathogens (Mhamdi and Noctor 2016; Zhou et al. 2017, 2019; Williams et al. 2018b). Changes in atmospheric CO<sub>2</sub> levels not only affect plant-pathogen interactions, but also impact the interaction of plants with mutualistic mycorrhizal fungi and plant growth-promoting rhizobacteria (Werner et al. 2018; Williams et al. 2018a). Hence, to produce climate resilient crops in the future, it is important to understand how changes in atmospheric CO<sub>2</sub> levels impact plant–microbe interactions.

Carbonic anhydrases (CAs) are metalloenzymes that were initially purified from red blood cells and mainly function as catalysts in the interconversion of CO<sub>2</sub> and bicarbonate (Meldrum and Roughton 1933). There are at least five distinct CA families ( $\alpha$ ,  $\beta$ ,  $\gamma$ ,  $\delta$ , and  $\epsilon$  CAs), three of which ( $\alpha$ ,  $\beta$ , and  $\gamma$  CAs) are ubiquitously distributed

among animal, plant, and bacterial species. The widespread distribution and abundance of these CA families underline their evolutionary importance throughout the kingdom of life.  $\beta$ CAs represent the most prominent group of CAs in plants. They are involved in a wide range of biological processes, including CO<sub>2</sub> homeostasis, stomatal aperture, respiration, photosynthesis, pH regulation, and anther cell differentiation (Henry 1996; Smith and Ferry 2000; Hu et al. 2010; Engineer et al. 2014; Huang et al. 2017). *Arabidopsis* contains six  $\beta$ CA genes (*At $\beta$ CA1-6*), which are mostly expressed in aboveground tissues (Wang et al. 2014). Several studies reported on the implication of CAs in plant defense. For instance, the expression of a plastidic CA gene was found to be repressed in potato leaves upon challenge with the potato late blight pathogen *Phytophthora infestans* (Restrepo et al. 2005). Similarly, expression of the CA gene *TC52686* in grapevine was suppressed during infection with the grapevine downy mildew pathogen *Plasmopara viticola* (Polesani et al. 2008). In contrast, five CA proteins were shown to be more abundant in a proteomic analysis of non-heading Chinese cabbage infected with the downy mildew *Hyaloperonospora parasitica* (Sun et al. 2014). These reported alterations in CA transcript or protein levels in pathogen-infected plants point to a potential role of CAs in plant defense. Indeed, a positive role in plant defense was demonstrated for a chloroplast-localized CA of tobacco, also known as SALICYLIC ACID (SA)-BINDING PROTEIN 3 (SABP3), as silencing of this CA gene in *Nicotiana benthamiana* leaves suppressed the hypersensitive response mediated by the *Pto:avrPto* resistance gene:effector gene pair (Slaymaker et al. 2002). Moreover, CA-silenced *N. benthamiana* was more susceptible to *P. infestans* than the wild type, supporting the notion that CAs contribute to disease resistance (Restrepo et al. 2005).

Despite the accumulating evidence for a role of CAs in plant immunity (Wang et al. 2009), little is known about how their regulation or action affects plant-pathogen interactions. CAs are mainly known as responders and actors in atmospheric CO<sub>2</sub>-mediated signaling. For example, under elevated CO<sub>2</sub> conditions, both transcript abundance and enzymatic activity of CAs have been shown to decrease in several plant species (Porter and Grodzinski 1984; Webber et al. 1994; Majeau and Coleman 1996). Moreover, stomatal closure under high CO<sub>2</sub> conditions and stomatal opening under low CO<sub>2</sub> conditions is hampered in the *Arabidopsis* CA double-mutant *calca4* (Hu et al. 2010). Stomata are entry points of many leaf pathogens. Since activation of PTI triggers the closure of stomata to prevent pathogen entry (Melotto et al. 2008), changes in CA-mediated stomatal aperture may impact disease resistance. Recently, Medina-Puche et al. (2017) reported that several *Arabidopsis* CAs interact with the transcriptional coregulator NONEXPRESSOR

OF PATHOGENESIS-RELATED GENES 1 (NPR1) and NONRECOGNITION OF BTH-4 (NRB4), thereby modulating the perception of the plant defense hormone salicylic acid (SA) in plants. SA is produced during the onset of PTI and plays an important regulatory role in plant immunity (Klessig et al. 2018). Hence, under changing atmospheric CO<sub>2</sub> conditions, CA-mediated changes in SA responses may have an effect on the level of disease resistance. Previous observations that SA-dependent defenses in Arabidopsis are modulated under changing atmospheric CO<sub>2</sub> conditions (Mhamdi and Noctor 2016; Williams et al. 2018b) support this hypothesis.

Given the importance of CA1 and CA4 in Arabidopsis' responsiveness to changing CO<sub>2</sub> levels (Hu et al. 2010), we chose to investigate the role of these two CAs in plant immunity and determined their effect on CO<sub>2</sub>-modulated defense using the model plant-pathogen system Arabidopsis *P. syringae*. We provide evidence that suppression of CA1 and CA4 gene expression is involved in the plant defense response to *P. syringae* infection and that CA1 and CA4 act as negative regulators of plant immunity, likely through antagonizing SA-mediated signaling. We also found that differential expression of CA1 under different atmospheric CO<sub>2</sub> conditions is correlated with an altered level of disease resistance against *P. syringae* and that CA1 and CA4 are required for the effects of CO<sub>2</sub> on disease resistance against *P. syringae*.

## Materials and methods

### Cultivation of plants and bacterial strains

For experiments with soil-grown plants, seeds of *Arabidopsis thaliana* accession Col-0 (Arabidopsis Biological Resource Center (ABRC) stock number CS1092) and mutant *calca4* (Hu et al. 2010; kindly provided by Julian Schroeder, UCSD, San Diego, CA, USA) were sown on autoclaved river sand. Two weeks later, seedlings were transferred to 60-ml pots containing a sand/potting soil mixture that was autoclaved twice for 20 min. Plants were grown in a climate chamber with a 10-h day at 20 °C and 14-h night at 18 °C cycle (350 μmol m<sup>-2</sup> s<sup>-1</sup>) with 70% relative humidity. For experiments with different atmospheric CO<sub>2</sub> treatments, 2-week-old seedlings in 60-ml pots either stayed in the growth room (ambient; 450 ppm) or were transferred to similar growth rooms with exactly the same conditions, except for CO<sub>2</sub> levels, which were high (800 ppm), or low (150 ppm; Zhou et al. 2017). Plants were grown for the remainder of the experiment under different CO<sub>2</sub> conditions. The technical specifications of the CO<sub>2</sub>-controlled growth chambers used in this study were described in detail by Temme et al. (2015).

For experiments with in vitro-grown plants, seeds of Arabidopsis accession Col-0 and mutants *aba2-1* (Koornneef et al. 1982; ABRC stock number CS156), *coi1-1* (Feys et al. 1994; kindly provided by Jane Glazebrook, University of Minnesota, St. Paul, MN, USA), *npr1-1* (Cao et al. 1994; ABRC stock number N3726), *ein2-1* (Guzman and Ecker 1990; ABRC stock number N3071), and *fls2* (Shan et al. 2008; ABRC stock number SALK\_141277) were surface sterilized in gas of a mixture of household chlorine (Glorix original, Unilever, Vlaardingen, the Netherlands) and HCl (37%; 97:3) for 3–4 h. Sterile seeds were subsequently sown on agar plates or in liquid. The agar plates contained Murashige and Skoog (MS) medium (Duchefa Biochemie, Haarlem, the Netherlands), pH 5.9, supplemented with 5 mM MES buffer, 10 g l<sup>-1</sup> sucrose and 0.85% (w/v) plant agar (Duchefa Biochemie). When plants were 2-weeks old, they were transferred to liquid medium to be treated with flg22 (see "MAMP treatment"). For experimental conditions in which seeds were sown immediately in liquid MS, see "MAMP treatment".

*Pseudomonas syringae* pv. *tomato* DC3000 (*Pst*) and its corresponding effector-deficient mutant *Pst hrpA*<sup>-</sup> (de Torres et al. 2003; Truman et al. 2006), and *Pseudomonas syringae* pv. *maculicola* ES4326 (*Psm*) and its corresponding coronatine-deficient mutant *Psm cor*<sup>-</sup> (Dong et al. 1991) were grown on King's B medium (King et al. 1954) agar plates supplemented with 50 μg ml<sup>-1</sup> rifampicine at 28 °C.

### *Pseudomonas syringae* inoculation and bioassay

*Pseudomonas syringae* inoculation and the disease resistance assay were performed as described (Van Wees et al. 2013). For dip inoculation, the bacterial inoculum was diluted to a final concentration of 5 × 10<sup>7</sup> cfu ml<sup>-1</sup> of 10 mM MgSO<sub>4</sub> containing 0.015% (v/v) Silwet L-77 (Van Meeuwen Chemicals, Weesp, the Netherlands). For pressure infiltration, the bacterial suspension was adjusted to a concentration of 4 × 10<sup>7</sup> cfu ml<sup>-1</sup> unless specified otherwise. Bacterial growth *in planta* was determined as described (Zhou et al. 2019). Eight biological replicates were included for each time point.

*Pseudomonas syringae* disease symptoms were scored in the following classes according to their severity: class 1, 0–10% chlorotic or water-soaked area per leaf; class 2, 10–50% chlorotic or water-soaked area per leaf; class 3, > 50% chlorotic or water-soaked area per leaf. Six fully grown and morphologically similar leaves per plant were chosen for scoring and 12 plants were scored per treatment. The average *P. syringae* disease index per plant was calculated using the formula:

$$\sum_{c=1}^3 (c \times \text{the number of leaves in class } c) / 6$$

$c$ , the value of the class (1, 2, or 3). The resulting continuous data were tested for normal distribution by the Shapiro–Wilk test and if they passed, they were subsequently subjected to parametric tests for statistical analysis as indicated in the legends.

### Botrytis cinerea bioassay

*Botrytis cinerea* strain B05.10 (Van Kan et al. 1997) was used for the inoculation of 4-week-old plants. Spore inoculation and disease resistance assay were performed as described previously (Van Wees et al. 2013; Zhou et al. 2019). Disease symptoms were scored at 3 days after inoculation. The average disease index was calculated similarly as described above for the *P. syringae* disease index.

### MAMP treatment

For gene expression analysis of plants treated with the MAMPs flg22 or nlp20, 2-week-old in vitro-grown seedlings were transferred from agar plates to 24-well plates containing 1.5 ml of liquid MS with 5 mM MES per well and kept overnight at room temperature. Subsequently, a solution of 0.5 ml of MS + MES supplemented with flg22 (Sigma), or nlp20 (kind gift of Thorsten Nürnberger, Universität Tübingen, Germany (Böhm et al. 2014)) was added to obtain the final concentration (as indicated in the figure legends). The rosette leaves or the whole seedlings were harvested for RNA extraction at indicated time points.

For the growth inhibition assay, seeds of Col-0 and *calca4* were surface sterilized and sown in 96-well plates with 200 µl liquid MS + MES per well, supplemented or not with flg22 (1, 10, or 100 nM) from a 100 mM stock solution of flg22. The dry weight was measured when the seedlings were 2-weeks old.

### ROS measurement

For the ROS assay, plants were grown at 20 °C in an 8-h light/16-h dark cycle in growth chambers. Leaf discs from 5-week-old plants were floated on water overnight. The water was replaced with 100 µl of a solution containing 20 µM luminol (Sigma), 1 µg horseradish peroxidase (Fluka, Buchs, Switzerland) and 100 nM flg22. ROS production was measured as previously described (Mersmann et al. 2010; Roux et al. 2011). Twelve leaf discs from 5-week-old plants were used for each condition. Luminescence of each sample was measured over 60 min continuously using a high-resolution

photon counting system (HRPCS218, Photek, East Sussex, UK) coupled to an aspherical wide lens (Sigma).

### Gene expression by qRT-PCR

Total RNA isolation and qRT-PCR were performed as described previously (Oñate-Sánchez and Vicente-Carbajosa 2008; Zhou et al. 2017), using the constitutively expressed reference gene *At1g13320* (Czechowski et al. 2005), encoding protein phosphatase PP2AA3, and the  $2^{-\Delta\Delta C_T}$  method (Schmittgen and Livak 2008) to calculate relative changes in gene expression. Three biological replicates were taken for each data point. Primers used for qRT-PCR are listed in Supplemental Table S1.

### Stomatal aperture measurement

To measure stomatal aperture, a modified protocol of dental resin impressions was used (Geisler et al. 2000; Zhou et al. 2017). Stomata were photographed under an Olympus microscope. Analysis D Olympus Software was used to examine the stomata on the pictures taken. Stomatal aperture was assessed by measuring the width and length of the stomata. At least 20–30 observations per leaf were recorded on at least six leaves per treatment.

## Results

### Repression of CA1 and CA4 expression upon infection by *P. syringae* independently of type-III effectors and coronatine

Transcriptional repression of *CA* genes in response to attack by diverse pathogens has been reported for various plant species. Genevestigator analysis (Zimmermann et al. 2004) of the six  $\beta$ -group members of the Arabidopsis *CA* genes shows that *CA1*, *CA2*, *CA4*, and *CA5* display a predominantly reduced expression pattern in response to infection by diverse plant pathogens, while *CA3* and *CA6* show a more variable profile (Supplemental Table S2). For this study, we chose to investigate the role of *CA1* and *CA4* in Arabidopsis immunity to *P. syringae* under ambient and altered CO<sub>2</sub> conditions, because of their previously reported role in CO<sub>2</sub>-mediated responses (Hu et al. 2010). We first monitored the expression of *CA1* and *CA4* upon *P. syringae* infection of Arabidopsis cultivated under ambient CO<sub>2</sub> conditions. In mock-infiltrated Col-0 leaves, *CA1* and *CA4* showed a similar basal expression pattern over time, in which the highest level was reached at 24 h after mock treatment (11:00 am) (Fig. 1a, b). This corroborates with a previously reported finding on diurnal rhythm of *CA* gene expression in *Chlamydomonas reinhardtii* (Fujiwara et al. 1996), which may



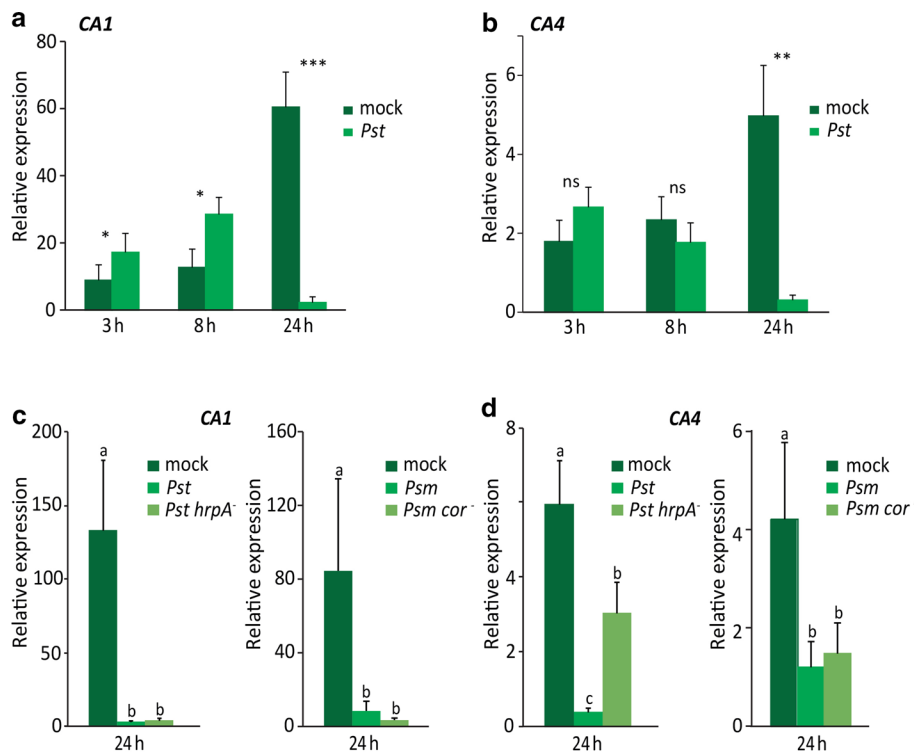


**Fig. 1** *Pseudomonas syringae* represses the expression of *CA1* and *CA4* independently of *hrpA*-dependent effectors and coronatine. **a** *CA1* and **b** *CA4* expression levels relative to the reference gene *At1g13320* in leaves of 4-week-old Col-0 plants at 3, 8, and 24 h after pressure infiltration with mock (10 mM MgSO<sub>4</sub>) or *Pst* (4 × 10<sup>6</sup> cfu ml<sup>-1</sup>). Asterisks indicate statistically significant differences between mock and *Pst* treatment at specific time points (Student's *t* test; \**P* < 0.05; \*\**P* < 0.001; \*\*\**P* < 0.0001; *ns* not

significant). **c** *CA1* and **d** *CA4* expression levels relative to the reference gene *At1g13320* in leaves of 4-week-old Col-0 at 24 h after pressure infiltration with mock (10 mM MgSO<sub>4</sub>), *Psm* or *Psm cor*<sup>-</sup> (1 × 10<sup>7</sup> cfu ml<sup>-1</sup>), or *Pst* or *Pst hrpA*<sup>-</sup> (1 × 10<sup>8</sup> cfu ml<sup>-1</sup>). Different letters indicate statistically significant differences between treatments (one-way ANOVA; Fisher's LSD test; *P* < 0.05). Error bars represent SD, *n* = 3 plants

be associated with diurnal variations in cellular CO<sub>2</sub> levels. At 24 h after pressure infiltration of Arabidopsis leaves with *Pst*, the expression levels of *CA1* and *CA4* were significantly suppressed in comparison to the mock treatment (Fig. 1a, b). Together with the Genevestigator results (Supplemental Table S2), these results suggest that repression of *CA* gene expression is a common plant response to pathogen infection.

*Pseudomonas syringae* produces a suite of effector molecules, including the phytotoxin coronatine, which act to suppress plant defenses and promote infection (Mittal and Davis 1995; Brooks et al. 2005; Dou and Zhou 2012). To determine whether these virulence factors have a role in the suppression of *CA* gene expression, we tested the effect of infection by a *Pst hrpA*<sup>-</sup> mutant, which is defective in the type-III secretion system that translocates effectors into the plant host cell, and a *Psm cor*<sup>-</sup> mutant, which is defective in coronatine production. We compared the *CA1* and *CA4* expression levels after infiltration of the leaves with the mutant strains versus their respective wild-type *P. syringae* strains *Pst* and *Psm*. Confirming the findings displayed in

Fig. 1a, b, *CA1* and *CA4* were significantly repressed 24 h after infection with wild-type *Pst* and *Psm* (Fig. 1c, d). Infection by the mutant strains *Pst hrpA*<sup>-</sup> and *Psm cor*<sup>-</sup> repressed *CA1* to the same extent as the respective wild-type *P. syringae* strains (Fig. 1c). Also, *CA4* expression was significantly suppressed by the *P. syringae* mutants, although the effect of *Pst hrpA*<sup>-</sup> was less pronounced than that of wild-type *Pst* (Fig. 1d). Together, this suggests that repression of *CA1* and *CA4* in Arabidopsis by infection with *P. syringae* is largely independent of effectors and coronatine.

**Suppression of CA gene expression is a MAMP-induced response**

Next, we tested whether the suppression of *CA* gene expression by *P. syringae* might be a MAMP-induced response. To this end, we examined the expression pattern of *CA1* and *CA4* in response to treatment with flg22, the 22-amino acid immunogenic epitope of the bacterial MAMP flagellin. As shown in Fig. 2a, the expression of the flg22-induced marker gene *FRK1* was significantly enhanced in Col-0 plants from

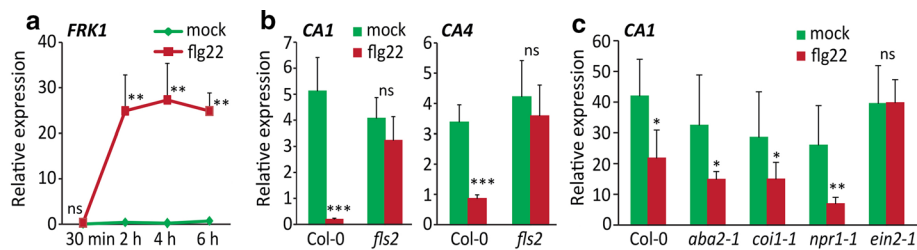


**Fig. 2** Expression of defense-related marker gene *FRK1* and *CA1* and *CA4* in response to flg22 treatment. **a** Expression of *FRK1* relative to the reference gene *At1g13320* in response to treatment with flg22 (500 nM) or water (mock) in 2-week-old Col-0 seedlings at specified time points after treatment (30 min and 2, 4, and 6 h). Asterisks indicate statistically significant differences between mock and flg22 treatment at specific time points (Student's *t* test; \* $P < 0.05$ ; \*\* $P < 0.01$ ; ns not significant). **b** *CA1* and *CA4* expression levels relative to the refer-

ence gene *At1g13320* in 2-week-old seedlings of Col-0 and *fls2*, 24 h after flg22 (125 nM) or mock treatment. **c** *CA1* expression levels relative to the reference gene *At1g13320* in 2-week-old seedlings of Col-0, *aba2-1*, *coi1-1*, *npr1-1*, and *ein2-1* at 8 h after flg22 (500 nM) or mock treatment. Asterisks indicate statistically significant differences between mock and flg22 treatment within each genotype (two-way ANOVA; Fisher's LSD test; \*\*\* $P < 0.001$ ; \*\* $P < 0.01$ ; \* $P < 0.05$ ; ns not significant). Error bars represent SD,  $n = 3$  plants

2 h after flg22 treatment onwards, indicating that the flg22 treatment had been effective. The expression of *CA1* and *CA4* was examined at 24 h after flg22 application in both wild-type Col-0 and the flg22 receptor mutant *fls2* (Gómez-Gómez and Boller 2000; Shan et al. 2008). At 24 h after flg22 application, both *CA1* and *CA4* were significantly suppressed in Col-0 plants, whereas this repression by flg22 was compromised in the *fls2* mutant (Fig. 2b). This indicates that the suppression of *CA* genes occurs downstream of the recognition of the MAMP flg22. Besides flg22, analysis of available Genevestigator microarray data also show repression of *CA1* and/or *CA4* by other defense elicitors, such as EF-Tu (elf18), necrosis-inducing *Phytophthora* protein 1 (NPP1), lipopolysaccharide (LPS), oligosaccharides (OGs), *Serratia plymuthica* HRO-C48 volatiles, and peptide 2 (Pep2; Supplementary Table S3). Also, the *Hyaloperonospora arabidopsidis* MAMPs necrosis and ethylene-inducing peptide (Nep1)-like proteins (HaNLPs) significantly repress *CA1* and *CA4* gene expression in Arabidopsis (Oome et al. 2014). Collectively, these results suggest that suppression of *CA1* and *CA4* gene expression is a general MAMP-induced response in Arabidopsis.

Plant hormones such as SA, ethylene (ET), jasmonic acid (JA), and abscisic acid (ABA) have all been implicated in the regulation of PTI (Tsuda and Katagiri 2010; Cao et al. 2011). To investigate whether these hormones play a role in MAMP-induced suppression of *CA* genes, we determined the expression of *CA1* in response to flg22 treatment in mutants impaired in synthesis of ABA (*aba2-1*), or responsiveness to JA (*coi1-1*), SA (*npr1-1*), or ET (*ein2-1*). We observed that the suppression of *CA1* by flg22 occurred to the same extent in the mutants *aba2-1*, *coi1-1*, and *npr1-1* as in wild-type Col-0 (Fig. 2c). In contrast, the *ein2-1* mutant did not display suppression of *CA1* gene expression in response to flg22 treatment; however, it has been demonstrated that ET signaling is required for the steady-state expression of the

Arabidopsis flg22 receptor gene *FLS2* (Boutrot et al. 2010; Mersmann et al. 2010). The lack of flg22-mediated suppression of *CA1* in *ein2* may, therefore, be explained by a diminished recognition of flg22 rather than diminished signaling downstream of recognition by *FLS2*. The results with the ABA-, JA-, and SA-related mutants suggest that ABA-, JA-, and SA-dependent signaling are not likely to be important for in flg22-mediated suppression of *CA1* gene expression.

### Enhanced MAMP responsiveness in mutant *ca1ca4*

After MAMP perception, multiple responses are activated (e.g. oxidative burst, stomatal closure, and SA accumulation), which are often accompanied by a substantial transcriptional reprogramming (Yu et al. 2017). To gain insight in the function of *CAs* in plant immunity, we examined several flg22-induced responses in the *ca1ca4* double mutant, which carries T-DNA insertions in the *CA1* and *CA4* genes (Hu et al. 2010). Figure 3a shows that flg22 induced *FRK1* to a significantly higher level in *ca1ca4* than in Col-0. Likewise, significantly augmented transcript levels of the SA biosynthesis gene *ICS1* were induced in the *ca1ca4* mutant after flg22 application (Fig. 3b). Transcript levels of the flg22 receptor gene *FLS2* remained unaltered in *ca1ca4* compared to Col-0 (Fig. 3c), indicating that the effects of *CA1* and *CA4* on defense-related gene expression are not due to differences in *FLS2* expression. Similar to flg22, the oomycete MAMP nlp20, which is the active 20-amino acid immunogenic epitope of HaNLPs (Böhm et al. 2014), also induced enhanced transcript levels of the SA-responsive genes *FRK1* (Fig. 3a) and *ICS1* in *ca1ca4* (Fig. 3b), suggesting that *CA1* and *CA4* broadly affect MAMP-induced transcription of the defense-related marker genes.

Flg22 treatment causes strong growth inhibition in Arabidopsis seedlings (Gómez-Gómez et al. 1999). To assay for flg22-mediated growth inhibition, Col-0 and *ca1ca4*

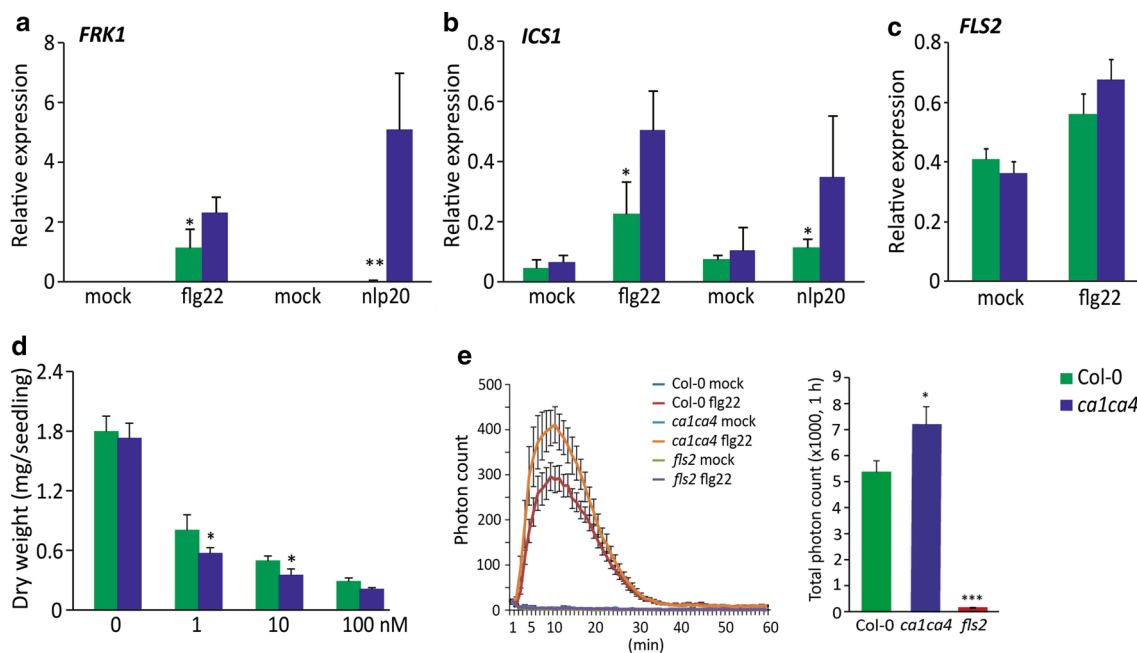


**Fig. 3** Augmented defense responses in the *calca4* mutant upon flg22 and nlp20 treatment. **a** *FRK1*, **b** *ICS1*, and **c** *FLS2* expression levels relative to the reference gene *At1g13320* in 2-week-old seedlings of wild-type Col-0 and mutant *calca4* plants at 24 h after flg22 (500 nM), nlp20 (100 nM) or mock treatment. Asterisks indicate statistically significant differences between Col-0 and *calca4* within the same treatment (Student’s *t* test; \**P* < 0.05; \*\**P* < 0.01). Error bars represent SD, *n* = 3 seedlings. **d** Dry weight of 2-week-old seedlings of Col-0 and *calca4* cultivated in the presence of 0, 1, 10, or 100 nM flg22. Depicted are the averages of dry weight per seedling. Asterisks indicate statistically significant differences between Col-0 and *calca4*

within the same treatment (Student’s *t* test; \**P* < 0.05). Error bars represent SD, *n* = 8 seedlings. **e** ROS burst induced by flg22 (100 nM) or mock treatment in leaf discs of Col-0, *calca4*, and *fls2*. Depicted in the left panel are photon counts in each genotype after mock or flg22 treatment at indicated time points after flg22 treatment. The right panel depicts cumulative ROS production (photon counts) within 1 h after flg22 treatment. Asterisks indicate statistically significant differences between mutants and wild-type Col-0 (one-way ANOVA, Fisher’s LSD test; \**P* < 0.05; \*\*\**P* < 0.001). Error bars represent SE, *n* = 4/12 (mock/flg22) leaf discs

seedlings were grown for 2 weeks in the presence of flg22 after which their dry weight was determined. Col-0 displayed more than 50% growth reduction after treatment of 1 nM flg22 (Fig. 3d). Interestingly, growth of *calca4* was reduced to a significantly greater extent than Col-0 after treatment with 1 nM and 10 nM flg22. Another feature of the flg22-induced defense response is the generation of reactive oxygen species (ROS; Nühse et al. 2007). The flg22-triggered ROS burst was significantly enhanced in the *calca4* mutant compared to that in Col-0 (Fig. 3e). Together, these results show that *calca4* plants display an augmented response to flg22 treatment, resulting in enhanced defense-related gene expression and a greater MAMP-mediated inhibition of seedling growth. From this, we conclude that CA1 and CA4 play a role in repressing MAMP-mediated defense responses.

**CA1 and CA4 reduce resistance to *Pst***

To further investigate the function of CAs in plant disease resistance, we tested the responsiveness of Col-0 and *calca4* to infection with *Pst*. Pathogen-induced stomatal

closure to inhibit pathogen entry has been established as an important defense response in plant resistance against *P. syringae* pathogens (Melotto et al. 2006). Therefore, we first determined whether CA1 and CA4, which are highly abundant in guard cells and control stomatal aperture (Hu et al. 2010), play a role in *Pst*-induced stomatal closure and opening. We tested stomatal responsiveness in Col-0 and *calca4* after treatment with *Pst* by dip inoculation, upon which the bacteria enter the leaf interior through stomatal openings. Consistent with previous results (Melotto et al. 2006), Col-0 plants reacted by closing their stomata between 1 and 2.5 h after *Pst* inoculation, and subsequent reopening at 4 h (Fig. 4a, b). As demonstrated previously (Hu et al. 2010), we observed that the stomatal aperture of *calca4* is significantly higher than that of Col-0 (Fig. 4a). Moreover, *Pst*-induced stomatal closure was delayed in *calca4* and became only apparent at 7 h after inoculation (Fig. 4a, b). The delayed stomatal closure triggered by *Pst* infection in *calca4* supports the notion that CA1 and CA4 are involved in *Pst*-induced stomatal movements.

Next, we performed disease resistance assays with Col-0 and *calca4* in which growth of *Pst* and disease symptoms

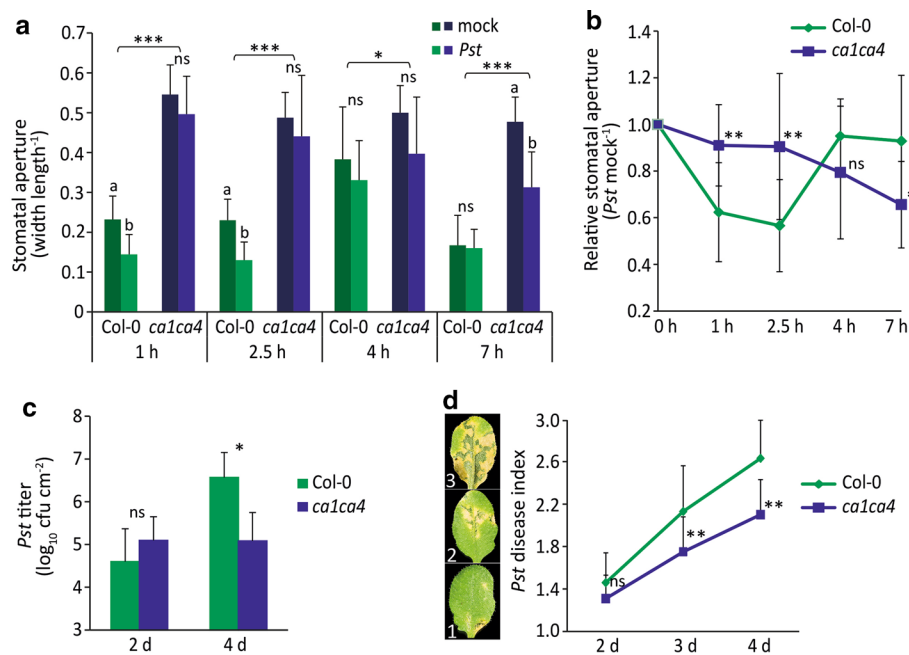


**Fig. 4** CA1 and CA4 influence stomatal aperture and resistance to *P. syringae*. **a** Stomatal aperture in leaves of 4-week-old wild-type Col-0 and mutant *calca4* plants at 1, 2.5, 4, and 7 h after dip inoculation with *Pst* ( $5 \times 10^7$  cfu ml $^{-1}$ ). Indicated are the averages of stomatal aperture ( $\pm$ SD) of six leaves. Different letters indicate statically significant differences between mock and *Pst* treatment within the same genotype (two-way ANOVA; Fisher's LSD test;  $P < 0.01$ ; *ns* not significant). Indications above the brackets specify whether there is an overall statistically significant difference between Col-0 and *calca4* at specific time points ( $***P < 0.001$ ;  $*P < 0.05$ ). Error bars represent SD,  $n = 6$  leaves. **b** Stomatal apertures in *Pst*-treated leaves relative to mock (10 mM MgSO $_4$ )-treated leaves at 0, 1, 2.5, 4, 7 h after treatment. Asterisks indicate statistically significant differences between Col-0 and *calca4* at specific time points (Student's *t* test;  $**P < 0.01$ ;  $*P < 0.05$ ; *ns* not significant). Error bars represent SD,  $n = 6$  leaves.

**c** Bacterial growth in 4-week-old Col-0 and *calca4* plants at 2 and 4 days after dip inoculation with *Pst* ( $5 \times 10^7$  cfu ml $^{-1}$ ). Indicated are the averages of log $_{10}$ -transformed bacterial titers per leaf area. Asterisks indicate statistically significant differences between Col-0 and *calca4* at specific time points (Student's *t* test;  $*P < 0.05$ ; *ns* not significant). Error bars represent SD,  $n = 8$  plants. **d** Disease symptom severity on 4-week-old Col-0 and *calca4* plants at 2, 3, and 4 days after pressure infiltration with *Pst* ( $6 \times 10^5$  cfu ml $^{-1}$ ). Indicated is the average of the disease index calculated from the percentage of leaves in three different disease severity classes. Class 1, 0–10% chlorotic or water-soaked area per leaf; class 2, 10–50% chlorotic or water-soaked area per leaf; class 3, >50% chlorotic or water-soaked area per leaf. Asterisks indicate statistically significant differences between Col-0 and *calca4* at specific time points (Student's *t* test;  $**P < 0.01$ ; *ns* not significant). Error bars represent SD,  $n = 12$  plants

were monitored. Double-mutant *calca4* exhibited a bacterial titer that was significantly lower than that of Col-0 plants at 4 d after dip inoculation with *Pst* (Fig. 4c). Plants were also inoculated with *Pst* by pressure infiltration, which bypasses stomatal defense. Figure 4d shows that the *calca4* mutant developed significantly fewer disease symptoms than Col-0 plants at 3 and 4 days after infiltration. Together, these results show that CA1 and CA4 negatively impact disease resistance to *Pst*, with no clear role for stomatal defense, suggesting that post-invasion defenses are antagonized.

### CA1 and CA4 antagonize SA-responsive gene expression upon *Pst* infection

In Arabidopsis, SA plays an important role in activating defense against *P. syringae* (Pieterse et al. 2012). To investigate whether CA1 and CA4 interfere with SA-dependent defenses, we infiltrated leaves of Col-0 and *calca4* plants

with *Pst* and subsequently monitored expression levels of the SA-responsive genes *PR1*, *PR2*, *FRK1*, *ICS1*, *WRKY22*, and *WRKY29*. Figure 5 shows that all tested SA-responsive genes were induced by *Pst* to a significantly higher level in *calca4* than in Col-0 and most of the genes showed a slightly enhanced basal expression level in the *calca4* mutant. Conversely, the JA-responsive marker gene *VSP2* was significantly suppressed in *Pst*-infected *calca4* plants (Fig. 5). These data suggest that CA1 and CA4 may modulate plant immunity by affecting SA- and JA-dependent plant responses.

### CA1 and CA4 are involved in atmospheric CO $_2$ -affected disease resistance against *Pst*

Atmospheric CO $_2$  levels have been shown to influence plant development and defense (Velasquez et al. 2018). In Arabidopsis, plant growth and the level of resistance against *P. syringae* is also impacted by changes in atmospheric CO $_2$



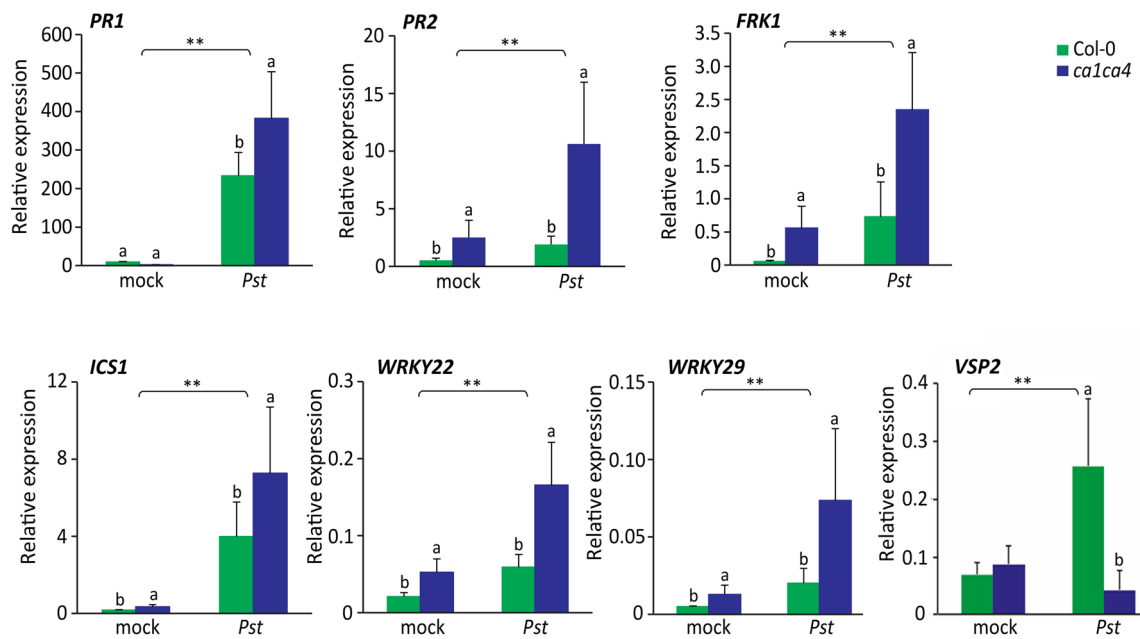


**Fig. 5** SA- and JA-responsive gene expression in the mutant *calca4* upon infection by *P. syringae*. *PR1*, *PR2*, *FRK1*, *ICS1*, *WRKY22*, *WRKY29*, and *VSP2* expression levels relative to the reference gene *At1g13320* in 4-week-old Col-0 and *calca4* plants 24 h after infiltration with *Pst* ( $4 \times 10^7$  cfu ml<sup>-1</sup>) or 10 mM MgSO<sub>4</sub> (mock). Error bars

represent SD,  $n=3$  plants. Different letters indicate statically significant differences between Col-0 and *calca4* within the same treatment (two-way ANOVA; Fisher’s LSD test;  $P < 0.05$ ). Indications above the brackets specify whether there is an overall statistically significant difference between mock and *Pst* treatment (\*\* $P < 0.01$ )

levels (Zhou et al. 2017, 2019). In the present study, we tested the role of CA1 and CA4 in the effect of changes in atmospheric CO<sub>2</sub> levels on Arabidopsis disease resistance against *Pst*. We found that the disease resistance of Arabidopsis Col-0 plants against *Pst* was decreased under

high CO<sub>2</sub> (800 ppm) compared with that under ambient CO<sub>2</sub> (450 ppm), whereas it was enhanced under low CO<sub>2</sub> conditions (150 ppm; Fig. 6a), confirming previous findings (Zhou et al. 2017). In the *calca4* double mutant, the level of *Pst* resistance was at all three atmospheric CO<sub>2</sub> levels as high as

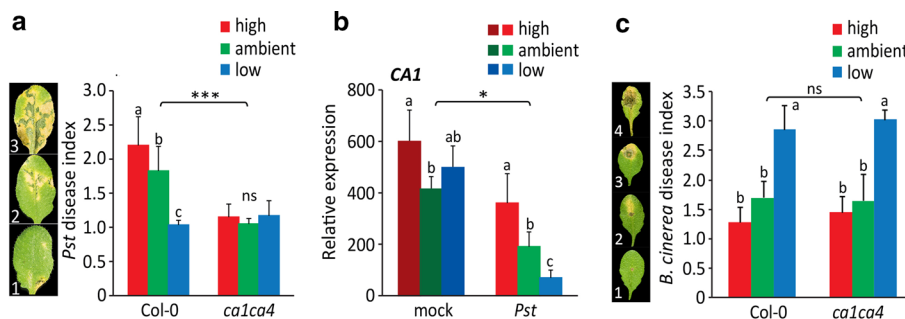


**Fig. 6** The role of CAs in atmospheric CO<sub>2</sub>-modulated disease resistance to *Pst* and *B. cinerea*. Arabidopsis wild-type Col-0 and mutant *calca4* plants were grown under high (800 ppm), ambient (450 ppm) and low (150 ppm) levels of atmospheric CO<sub>2</sub> until 4-week old and dip inoculated with *Pst* (a, b) or drop inoculated with *B. cinerea* (c). a Disease severity in Col-0 and *calca4* at 4 d after dip inoculation with *Pst* ( $4 \times 10^7$  cfu ml<sup>-1</sup>). Shown is the average *Pst* disease index calculated from the percentage of six leaves per plant belonging to different disease severity classes. Error bars represent SD,  $n=12$  plants. b *CA1* expression levels relative to the reference gene *At1g13320* in Col-0 grown under high, ambient and low levels of atmospheric CO<sub>2</sub> at 24 h after dip inoculation with *Pst*

( $1 \times 10^8$  cfu ml<sup>-1</sup>) or 10 mM MgSO<sub>4</sub> (mock). Error bars represent SD,  $n=3$  plants. c Disease severity in Col-0 and *calca4* plants inoculated with *B. cinerea* ( $1 \times 10^6$  spores ml<sup>-1</sup>). Disease symptoms were scored 4 days after inoculation. Shown is the average of the disease index calculated from the percentage of leaves in four different disease severity classes. Error bars represent SD,  $n=12$  plants. Different letters indicate statistically significant differences between CO<sub>2</sub> treatments within the same genotype. Indications above the brackets specify the interaction (Arabidopsis genotype  $\times$  CO<sub>2</sub> conditions) between Col-0 and *calca4* and the three CO<sub>2</sub> conditions (two-way ANOVA; Fisher’s LSD test; \* $P < 0.05$ ; \*\*\* $P < 0.001$ ; ns not significant).

that observed in Col-0 under low CO<sub>2</sub> (Fig. 6a), suggesting that in wild-type plants, the CAs play a role in the modulation of atmospheric CO<sub>2</sub>-affected disease resistance to *Pst*. This was confirmed by the observation that the *Pst*-mediated suppression of *CA1* gene expression becomes stronger with decreasing CO<sub>2</sub> concentrations in the atmosphere (Fig. 6b).

In Arabidopsis, changes in atmospheric CO<sub>2</sub> levels can also affect disease resistance against necrotrophic fungi (Williams et al. 2018b; Zhou et al. 2019). To test whether CAs play a role in this process, we tested the resistance of Arabidopsis plants to the necrotrophic pathogen *B. cinerea* at three different atmospheric CO<sub>2</sub> levels. We found that high CO<sub>2</sub>-grown Col-0 plants developed less disease symptoms compared with plants grown under ambient and low CO<sub>2</sub> conditions (Fig. 6c), confirming that Arabidopsis disease resistance against *B. cinerea* increases as atmospheric CO<sub>2</sub> levels increase (Zhou et al. 2019). Mutant *calca4* also displayed increasing levels of disease severity with increasing CO<sub>2</sub> levels, which was similar to that observed in Col-0 (Fig. 6c), suggesting that CA1 and CA4 do not influence atmospheric CO<sub>2</sub>-altered disease resistance to *B. cinerea*.

## Discussion

During the last decade, our understanding of the mechanisms involved in plant immune signaling greatly increased (Couto and Zipfel 2016; Cheng et al. 2019; Nobori and Tsuda 2019). Evidence is accumulating that climate change parameters can have profound effects on plant immunity (Noctor and Mhamdi 2017; Kazan 2018; Velasquez et al. 2018). As one of the core characteristics of global climate change, the increasing atmospheric CO<sub>2</sub> level has been shown to affect various plant-pathogen systems (Chakraborty et al. 2000; Garrett et al. 2006; Yáñez-López et al. 2014). In the present study, we revealed that the  $\beta$ -carbonic anhydrases CA1 and CA4 of Arabidopsis modulate plant immune responses and that they are likely involved in CO<sub>2</sub>-modulated plant defense against *Pst*.

Upon *P. syringae* infection, expression of the *CA1* and *CA4* genes in Arabidopsis was strongly repressed (Fig. 1). This occurred largely independently of *hrpA*-dependent effectors and coronatine (Fig. 1c, d). We further demonstrated that repression of *CA1* and *CA4* is triggered by the MAMPs *flg22* and *nlp20* (Fig. 2). This suggests that repression of *CA1* and *CA4* is part of the Arabidopsis defense response when under attack by *P. syringae*. The inability of the *ein2-1* mutant to repress *CA1* expression (Fig. 2c) most likely results from the strongly reduced expression of *FLS2* in *ein2-1* (Boutrot et al. 2010; Mersmann et al. 2010). However, a role for ET signaling in repression of *CA1* expression downstream of *flg22* recognition cannot be ruled out.

Nonetheless, the repression of *CA1* by *flg22* occurred independently of ABA, JA, or SA signaling (Fig. 2c).

In Arabidopsis, perception of *flg22* triggers multiple responses, such as activation of defense-related genes and growth inhibition (Yu et al. 2017). Our results with the double-mutant *calca4* show significantly enhanced expression levels of two defense-related marker genes, *FRK1* and *ICS1*, as well as stronger growth inhibition compared to wild-type plants upon treatment with *flg22* (Fig. 3). The *FLS2* expression levels were unaffected by the *calca4* mutation (Fig. 3c), suggesting the enhanced activation of plant immune responses by *flg22* is not likely due to an enhanced capacity of *flg22* recognition. This is supported by the observation that another MAMP, *nlp20*, also triggered enhanced expression of the defense-related marker genes *FRK1* and *ICS1* in *calca4* (Fig. 3a, b). Collectively, these data indicate that suppression of CAs is part of the basal plant immune response, thereby positively contributing to the activation of defenses against the pathogen encountered.

CAs have been reported to control CO<sub>2</sub> homeostasis and stomatal aperture. Consistent with previous findings (Henry 1996; Smith and Ferry 2000; Hu et al. 2010), our results showed that the *calca4* mutant displayed greater stomatal aperture than wild-type Col-0 plants (Fig. 4a). Moreover, stomatal closure, which is part of the defense response induced upon inoculation with *Pst*, is delayed in *calca4* as it is detected starting at 4 h while in Col-0, closure is already evident at 1 h after inoculation (Fig. 4a, b). This points to a positive role of the CAs in stomatal defenses. However, despite the larger opening of the stomata throughout the first 7 h and the delay in the stomatal closure response, the *calca4* mutant exhibited enhanced resistance to *Pst* compared to wild-type Col-0 in both the *Pst* dipping and infiltration assays (Fig. 4c, d). Although CA1 and CA4 positively regulate stomatal defenses, these results suggest that they negatively influence other post-invasion plant defense responses, likely those mediated by SA signaling, as the *calca4* mutant showed significantly augmented SA-responsive gene expression upon infection with *Pst* (Fig. 5).

Previous studies have shown a positive involvement of CAs in plant defense against avirulent *Pst* strains. For instance, in tobacco, silencing of the CA known as SA-BINDING PROTEIN 3 (SABP3), led to suppression of the *Pto:avrPto*-mediated hypersensitive defense response (Slaymaker et al. 2002). Also in Arabidopsis, the orthologue AtSABP3, which is also named CA1 (used in this study), is required for expression of full defense against the avirulent bacterial pathogen *Pst* carrying *avrB* (Wang et al. 2009). Our results showed that *CA1* gene expression was similarly repressed upon infection by wild-type *Pst* and its correspondent effector mutant *Pst hrpA*<sup>-</sup> (Fig. 1c). Still, the CA1 protein could be a potential target of type-III effectors of *Pst* as the abundance of CA1 was shown to be reduced to

a lesser extent upon infection by wild-type *Pst* than by its correspondent effector mutant *Pst hrpA*<sup>-</sup> (Jones et al. 2006). The dual role of CAs in defense against virulent and avirulent *Pst* strains suggests differential actions of CAs during compatible and incompatible interactions between a host and its pathogens.

One important aspect of prevailing climate changes is the elevation of atmospheric CO<sub>2</sub> and this has boosted research on plant defenses under elevated CO<sub>2</sub> conditions (Restrepo et al. 2005; Polesani et al. 2008; Noctor and Mhamdi 2017; Kazan 2018; Velasquez et al. 2018; Williams et al. 2018b). CAs are important enzymes in CO<sub>2</sub> metabolism and we addressed whether they play a role in atmospheric CO<sub>2</sub>—affected plant disease resistance. Previous reports have shown that elevated CO<sub>2</sub> increased the disease resistance of tomato plants against *Pst* (Li et al. 2014; Zhang et al. 2015). In contrast, we found enhanced disease susceptibility to *P. syringae* and increased resistance against *B. cinerea* in Arabidopsis plants grown at increasing CO<sub>2</sub> levels (Fig. 6; Zhou et al. 2017, 2019). This suggests that the response of plants to changes in the level of atmospheric CO<sub>2</sub> is plant species specific.

Arabidopsis defense against *P. syringae* and *B. cinerea* is largely regulated by SA and JA signaling, respectively (Glazebrook 2005). Previously, we showed that increasing atmospheric CO<sub>2</sub> levels lowered the level of resistance against *Pst*, while the level of resistance against *B. cinerea* increased (Zhou et al. 2019). This opposite effect on resistance against the (hemi)biotroph *Pst* and the necrotroph *B. cinerea* is likely due to the antagonistic interaction between the SA and the JA defense pathways (Pieterse et al. 2012). In this study, we confirmed our previous observation that with increasing CO<sub>2</sub> levels, Arabidopsis resistance against *Pst* decreases, while resistance against *B. cinerea* increases (Fig. 6). Moreover, we show that in mutant *calca4*, the effect of the atmospheric CO<sub>2</sub> level on *Pst* resistance is lost, while for *B. cinerea*, the CO<sub>2</sub> effect on resistance remains unaltered in comparison to Col-0 (Fig. 6). These results suggest that CAs predominantly have an impact on SA-mediated resistance.

Williams et al. (2018b) also tested the effect of both elevated and sub-ambient levels of atmospheric CO<sub>2</sub> on disease caused by necrotrophic (*Plectosphaerella cucumerina*) and biotrophic (*H. arabidopsidis*) pathogens. They observed enhanced resistance against the necrotroph under elevated CO<sub>2</sub> conditions, corroborating our findings with *B. cinerea* (Fig. 6c). However, in contrast to our observations, resistance against the biotroph was also enhanced under elevated CO<sub>2</sub> conditions. Similar observations were done by Mhamdi and Noctor (2016) who found enhanced resistance against both *Pst* and *B. cinerea* under conditions of elevated CO<sub>2</sub>. However, in the latter, study plants were grown at long day conditions (16 h light/8 h dark versus 10 h light/14 h dark

in our study) and at very high CO<sub>2</sub> levels (3000 ppm versus 800 ppm in our study), suggesting that effects of CO<sub>2</sub> on pathogen resistance are conditionally determined by prevailing environmental factors. Interestingly, both Williams et al. (2018b) and Mhamdi and Noctor (2016) provided evidence that the effect of changed atmospheric CO<sub>2</sub> levels on plant immunity is associated with cellular redox status. We found that the mutant *calca4* developed a stronger oxidative burst in response to flg22 treatment than did wild-type plants (Fig. 3e), confirming the notion that CAs may modulate plant immunity via changes in cellular redox processes. Different atmospheric CO<sub>2</sub> levels may also directly affect the growth rate or pathogenicity of the microbial pathogens, but we did not test to what extent this contributed to the disease outcome in our experiments.

In conclusion, our results show that induction of defense responses in *P. syringae*-infected Arabidopsis plants results in the repression of *CA1* and *CA4* gene expression. This leads to the alleviation of CA-mediated suppression of SA-dependent defenses and consequently increased disease resistance against *Pst* (Fig. 7). Changes in atmospheric CO<sub>2</sub> influence CA activity, which as a result impact SA-dependent defenses against *Pst*, possibly via changes in the cellular redox status (Mhamdi and Noctor 2016). Collectively, our results provide new leads for future investigations on plant adaptation to global environmental changes. A more

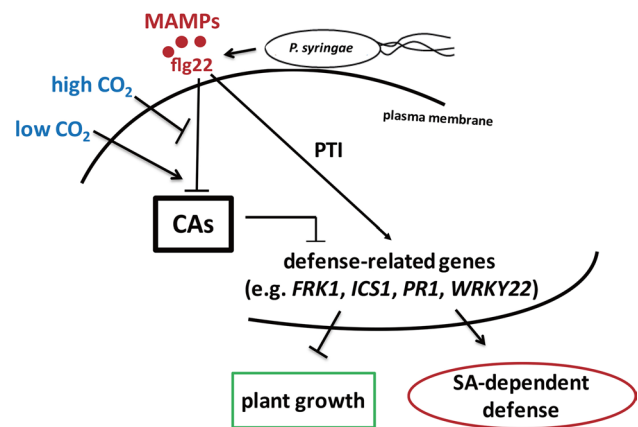


**Fig. 7** A model of CO<sub>2</sub>-modulated, MAMP-induced suppression of CA1 and CA4 that alleviate attenuation of SA-dependent defenses during the plant immune response to infection by *P. syringae*. Upon attack by *P. syringae*, plants recognize the flg22 epitope of the MAMP flagellin, resulting in repression of *CA1* and *CA4* gene expression. In uninduced plants, CAs have an antagonizing effect on PTI-mediated responses. Recognition of flg22 results in suppression of CAs and increased defense-related gene expression, ultimately leading to enhancement of SA-dependent resistance to *P. syringae* and inhibition of plant growth. At a low atmospheric CO<sub>2</sub> level, repression of *CA1* by *Pst* is enhanced, while at a high CO<sub>2</sub> level, *CA1* repression is reduced. This contributes to an increase versus a decrease in resistance levels against *Pst* at low and high CO<sub>2</sub> levels, respectively. Arrows, induction; blocked lines, repression

comprehensive analysis of the exact function of CAs in plant defense, including the  $\beta$ CAs that were not investigated here, will be subject of future study.

**Author contribution statement** YZ and SCMVW designed the experiments. YZ performed most of experiments and analyzed the data. Other authors assisted in experiments and discussed the results. YZ, IAV-V, CMJP, and SCMVW wrote the manuscript.

**Acknowledgements** We thank Dr Jane Glazebrook for the *Psm* and *Psm cor<sup>-</sup>* bacteria. This work was supported by a China Scholarship Council (CSC) PhD scholarship (to Y.Z.), VIDI Grant no. 11281 of the Netherlands Organization for Scientific Research (NWO/STW to S.C.M.V.W.), a grant from the Gatsby Charitable Foundation (to C.Z.), a long-term post-doctoral fellowship from the European Molecular Biology Organization (ALTF 657-2013; to D.V.d.D), and ERC Advanced Investigator Grant no. 269072 of the European Research Council (to C.M.J.P).

**Open Access** This article is licensed under a Creative Commons Attribution 4.0 International License, which permits use, sharing, adaptation, distribution and reproduction in any medium or format, as long as you give appropriate credit to the original author(s) and the source, provide a link to the Creative Commons licence, and indicate if changes were made. The images or other third party material in this article are included in the article's Creative Commons licence, unless indicated otherwise in a credit line to the material. If material is not included in the article's Creative Commons licence and your intended use is not permitted by statutory regulation or exceeds the permitted use, you will need to obtain permission directly from the copyright holder. To view a copy of this licence, visit <http://creativecommons.org/licenses/by/4.0/>.

## References

- Böhm H, Albert I, Oome S, Raaymakers TM, Van den Ackerveken G, Nürnberger T (2014) A conserved peptide pattern from a widespread microbial virulence factor triggers pattern-induced immunity in *Arabidopsis*. *PLoS Path* 10:e1004491
- Boutrot F, Segonzac C, Chang KN, Qiao H, Ecker JR, Zipfel C, Rathjen JP (2010) Direct transcriptional control of the *Arabidopsis* immune receptor FLS2 by the ethylene-dependent transcription factors EIN3 and EIL1. *Proc Natl Acad Sci USA* 107:14502–14507
- Brooks DM, Bender CL, Kunkel BN (2005) The *Pseudomonas syringae* phytotoxin coronatine promotes virulence by overcoming salicylic acid-dependent defences in *Arabidopsis thaliana*. *Mol Plant Pathol* 6:629–639
- Cao H, Bowling SA, Gordon AS, Dong X (1994) Characterization of an *Arabidopsis* mutant that is nonresponsive to inducers of systemic acquired resistance. *Plant Cell* 6:1583–1592
- Cao F, Yoshioka K, Desveaux D (2011) The roles of ABA in plant–pathogen interactions. *J Plant Res* 124:489–499
- Chakraborty S, Tiedemann A, Teng P (2000) Climate change: potential impact on plant diseases. *Environ Pollut* 108:317–326
- Cheng YT, Zhang L, He SY (2019) Plant-microbe interactions facing environmental challenge. *Cell Host Microbe* 26:183–192
- Couto D, Zipfel C (2016) Regulation of pattern recognition receptor signalling in plants. *Nat Rev Immunol* 16:537–552
- Czechowski T, Stitt M, Altmann T, Udvardi MK, Scheible W-R (2005) Genome-wide identification and testing of superior reference genes for transcript normalization in *Arabidopsis*. *Plant Physiol* 139:5–17
- Dong X, Mindrinos M, Davis KR, Ausubel FM (1991) Induction of *Arabidopsis* defense genes by virulent and avirulent *Pseudomonas syringae* strains and by a cloned avirulence gene. *Plant Cell* 3(1):61–72. <https://doi.org/10.1105/tpc.3.1.61>
- Dou D, Zhou J-M (2012) Phytopathogen effectors subverting host immunity: different foes, similar battleground. *Cell Host Microbe* 12:484–495
- de Torres M, Sanchez P, Fernandez-Delmond I, Grant M (2003) Expression profiling of the host response to bacterial infection the transition from basal to induced defense responses. *Plant J* 33:665–676
- Eastburn DM, Degennaro MM, Delucia EH, Dermody O, Mcelrone AJ (2010) Elevated atmospheric carbon dioxide and ozone alter soybean diseases at SoyFACE. *Glob Change Biol* 16:320–330
- Engineer C, Ghassemian M, Anderson J, Peck S, Hu H, Schroeder J (2014) Carbonic anhydrases, *EPF2* and a novel protease mediate CO<sub>2</sub> control of stomatal development. *Nature* 513:246–250
- Feys BJ, Benedetti CE, Penfold CN, Turner JG (1994) *Arabidopsis* mutants selected for resistance to the phytotoxin coronatine are male sterile, insensitive to methyl jasmonate, and resistant to a bacterial pathogen. *Plant Cell* 6:751–759
- Fujiwara S, Ishida N, Tsuzuki M (1996) Circadian expression of the carbonic anhydrase gene, *Cah1*, in *Chlamydomonas reinhardtii*. *Plant Mol Biol* 32:745–749
- Garrett KA, Dendy SP, Frank EE, Rouse MN, Travers SE (2006) Climate change effects on plant disease: genomes to ecosystems. *Annu Rev Phytopathol* 44:489–509
- Geisler M, Nadeau J, Sack FD (2000) Oriented asymmetric divisions that generate the stomatal spacing pattern in *Arabidopsis* are disrupted by the *too many mouths* mutation. *Plant Cell* 12:2075–2086
- Glazebrook J (2005) Contrasting mechanisms of defense against biotrophic and necrotrophic pathogens. *Annu Rev Phytopathol* 43:205–227
- Gómez-Gómez L, Boller T (2000) FLS2: An LRR receptor-like kinase involved in the perception of the bacterial elicitor flagellin in *Arabidopsis*. *Mol Cell* 5:1003–1012
- Gómez-Gómez L, Felix G, Boller T (1999) A single locus determines sensitivity to bacterial flagellin in *Arabidopsis thaliana*. *Plant J* 18:277–284
- Guzman P, Ecker JR (1990) Exploiting the triple response of *Arabidopsis* to identify ethylene-related mutants. *Plant Cell* 2:513–523
- Henry RP (1996) Multiple roles of carbonic anhydrase in cellular transport and metabolism. *Annu Rev Physiol* 58:523–538
- Hu H, Boisson Dernier A, Israelsson Nordström M, Böhmer M, Xue S, Ries A, Godoski J, Kuhn JM, Schroeder JI (2010) Carbonic anhydrases are upstream regulators of CO<sub>2</sub>-controlled stomatal movements in guard cells. *Nat Cell Biol* 12:87–93
- Huang J, Li Z, Biener G, Xiong E, Malik S, Eaton N, Zhao CZ, Raicu V, Kong H, Zhao D (2017) Carbonic anhydrases function in anther cell differentiation downstream of the receptor-like kinase EMS1. *Plant Cell* 29:1335–1356
- Jones AM, Thomas V, Bennett MH, Mansfield J, Grant M (2006) Modifications to the *Arabidopsis* defense proteome occur prior to significant transcriptional change in response to inoculation with *Pseudomonas syringae*. *Plant Physiol* 142:1603–1620
- Kazan K (2018) Plant-biotic interactions under elevated CO<sub>2</sub>: a molecular perspective. *Environ Exp Bot* 153:249–261
- King EO, Ward MK, Raney DE (1954) Two simple media for the demonstration of pyocyanin and fluorescein. *J Lab Clin Med* 44:301–307



- Klessig DF, Choi HW, Dempsey DA (2018) Systemic acquired resistance and salicylic acid: past, present, and future. *Mol Plant Microbe Interact* 31:871–888
- Koornneef M, Jorna M, Brinkhorst-Van der Swan D, Karssen C (1982) The isolation of abscisic acid (ABA) deficient mutants by selection of induced revertants in non-germinating gibberellin sensitive lines of *Arabidopsis thaliana* (L.) Heynh. *Theor Appl Genet* 61:385–393
- Li X, Sun Z, Shao S, Zhang S, Ahammed GJ, Zhang G, Jiang Y, Zhou J, Xia X, Zhou Y, Yu J, Shi K (2014) Tomato-*Pseudomonas syringae* interactions under elevated CO<sub>2</sub> concentration: the role of stomata. *J Exp Bot* 66:307–316
- Majean N, Coleman JR (1996) Effect of CO<sub>2</sub> concentration on carbonic anhydrase and ribulose-1, 5-bisphosphate carboxylase/oxygenase expression in pea. *Plant Physiol* 112:569–574
- Matros A, Amme S, Kettig B, Buck-Sorlin GH, Sonnewald U, Mock H-P (2006) Growth at elevated CO<sub>2</sub> concentrations leads to modified profiles of secondary metabolites in tobacco cv. Samsun NN and to increased resistance against infection with *potato virus Y*. *Plant Cell Environ* 29:126–137
- Medina-Puche L, Castello M, Canet J, Lamilla J, Colombo M, Tornero P (2017)  $\beta$ -carbonic anhydrases play a role in salicylic acid perception in *Arabidopsis*. *PLoS ONE* 12:e0181820
- Meldrum NU, Roughton FJW (1933) Carbonic anhydrase. Its preparation and properties. *J Physiol* 80:113–142
- Melloy P, Aitken E, Luck J, Chakraborty S, Obanon F (2014) The influence of increasing temperature and CO<sub>2</sub> on Fusarium crown rot susceptibility of wheat genotypes at key growth stages. *Eur J Plant Pathol* 140:19–37
- Melotto M, Underwood W, Koczan J, Nomura K, He SY (2006) Plant stomata function in innate immunity against bacterial invasion. *Cell* 126:969–980
- Melotto M, Underwood W, He S-Y (2008) Role of stomata in plant innate immunity and foliar bacterial diseases. *Annu Rev Phytopathol* 46:101–122
- Mersmann S, Bourdais G, Rietz S, Robatzek S (2010) Ethylene signaling regulates accumulation of the FLS2 receptor and is required for the oxidative burst contributing to plant immunity. *Plant Physiol* 154:391–400
- Mhamdi A, Noctor G (2016) High CO<sub>2</sub> primes plant biotic stress defences through redox-linked pathways. *Plant Physiol* 172:929–942
- Mittal S, Davis KR (1995) Role of the phytotoxin coronatine in the infection of *Arabidopsis thaliana* by *Pseudomonas syringae* pv. *tomato*. *Mol Plant Microbe Interact* 8:165–171
- Nobori T, Tsuda K (2019) The plant immune system in heterogeneous environments. *Curr Opin Plant Biol* 50:58–66
- Noctor G, Mhamdi A (2017) Climate change, CO<sub>2</sub>, and defense: the metabolic, redox, and signaling perspectives. *Trends Plant Sci* 22:857–870
- Nühse TS, Bottrill AR, Jones AME, Peck SC (2007) Quantitative phosphoproteomic analysis of plasma membrane proteins reveals regulatory mechanisms of plant innate immune responses. *Plant J* 51:931–940
- Oñate-Sánchez L, Vicente-Carbajosa J (2008) DNA-free RNA isolation protocols for *Arabidopsis thaliana*, including seeds and siliques. *BMC Res Notes* 1:93
- Oome S, Raaymakers TM, Cabral A, Samwel S, Böhm H, Albert I, Nürnberger T, Van den Ackerveken G (2014) Nep1-like proteins from three kingdoms of life act as a microbe-associated molecular pattern in *Arabidopsis*. *Proc Natl Acad Sci USA* 111:16955–16960
- Pieterse CMJ, Van der Does D, Zamioudis C, Leon-Reyes A, Van Wees SCM (2012) Hormonal modulation of plant immunity. *Annu Rev Cell Dev Biol* 28:489–521
- Polesani M, Desario F, Ferrarini A, Zamboni A, Pezzotti M, Kortekamp A, Polverari A (2008) cDNA-AFLP analysis of plant and pathogen genes expressed in grapevine infected with *Plasmopara viticola*. *BMC Genomics* 9:142
- Porter MA, Grodzinski B (1984) Acclimation to high CO<sub>2</sub> in bean carbonic anhydrase and ribulose bisphosphate carboxylase. *Plant Physiol* 74:413–416
- Restrepo S, Myers K, Del Pozo O, Martin G, Hart A, Buell C, Fry W, Smart C (2005) Gene profiling of a compatible interaction between *Phytophthora infestans* and *Solanum tuberosum* suggests a role for carbonic anhydrase. *Mol Plant Microbe Interact* 18:913–922
- Roux N, Schwessinger B, Albrecht C, Chinchilla D, Jones A, Holton M, Malinovsky FG, Tör M, De Vries S, Zipfel C (2011) The *Arabidopsis* leucine-rich repeat receptor-like kinases BAK1/SERK3 and BKK1/SERK4 are required for innate immunity to hemibiotrophic and biotrophic pathogens. *Plant Cell* 23:2440–2455
- Schmittgen TD, Livak KJ (2008) Analyzing real-time PCR data by the comparative C<sub>T</sub> method. *Nat Protoc* 3:1101–1108
- Shan LB, He P, Li JM, Heese A, Peck SC, Nürnberger T, Martin GB, Sheen J (2008) Bacterial effectors target the common signaling partner BAK1 to disrupt multiple MAMP receptor-signaling complexes and impede plant immunity. *Cell Host Microbe* 4:17–27
- Slaymaker DH, Navarre DA, Clark D, del Pozo O, Martin GB, Klessig DF (2002) The tobacco salicylic acid-binding protein 3 (SABP3) is the chloroplast carbonic anhydrase, which exhibits antioxidant activity and plays a role in the hypersensitive defense response. *Proc Natl Acad Sci USA* 99:11640–11645
- Smith KS, Ferry JG (2000) Prokaryotic carbonic anhydrases. *FEMS Microbiol Rev* 24:335–366
- Sun C, Wang L, Hu D, Riquicho ARM, Liu T, Hou X, Li Y (2014) Proteomic analysis of non-heading Chinese cabbage infected with *Hyaloperonospora parasitica*. *J Proteomics* 98:15–30
- Temme AA, Liu JC, Cornwell WK, Cornelissen JHC, Aerts R (2015) Winners always win: growth of a wide range of plant species from low to future high CO<sub>2</sub>. *Ecol Evol* 5:4949–4961
- Truman W, Zabala MT, Grant M (2006) Type III effectors orchestrate a complex interplay between transcriptional networks to modify basal defence responses during pathogenesis and resistance. *Plant J* 46:14–33
- Tsuda K, Katagiri F (2010) Comparing signaling mechanisms engaged in pattern-triggered and effector-triggered immunity. *Curr Opin Plant Biol* 13:459–465
- Van Kan J, Van't Klooster J, Wagemakers C, Dees D, Van der Vlugt-Bergmans C (1997) Cutinase A of *Botrytis cinerea* is expressed, but not essential, during penetration of gerbera and tomato. *Mol Plant Microbe Interact* 10:30–38
- Van Wees SCM, Van Pelt JA, Bakker PAHM, Pieterse CMJ (2013) Bioassays for assessing jasmonate-dependent defenses triggered by pathogens, herbivorous insects, or beneficial rhizobacteria. *Meth Mol Biol* 1011:35–49
- Velasquez A, Castroverde C, He S (2018) Plant-pathogen warfare under changing climate conditions. *Curr Biol* 28:619–634
- Wang YQ, Feechan A, Yun BW, Shafiei R, Hofmann A, Taylor P, Xue P, Yang FQ, Xie ZS, Pallas JA, Chu CC, Loake GJ (2009) S-Nitrosylation of AtSABP3 antagonizes the expression of plant immunity. *J Biol Chem* 284:2131–2137
- Wang M, Zhang Q, Liu FC, Xie WF, Wang GD, Wang J, Gao QH, Duan K (2014) Family-wide expression characterization of *Arabidopsis* beta-carbonic anhydrase genes using qRT-PCR and Promoter: GUS fusions. *Biochimie* 97:219–227
- Webber AN, Nie GY, Long SP (1994) Acclimation of photosynthetic proteins to rising atmospheric CO<sub>2</sub>. *Photosynth Res* 39:413–425
- Werner GDA, Zhou YL, Pieterse CMJ, Kiers ET (2018) Tracking plant preference for higher-quality mycorrhizal symbionts under varying CO<sub>2</sub> conditions over multiple generations. *Ecol Evol* 8:78–87



- Williams A, Petriacq P, Beetling D, Cotton T, Ton J (2018a) Impacts of atmospheric CO<sub>2</sub> and soil nutritional value on plant responses to rhizosphere colonization by soil bacteria. *Front Plant Sci* 9:1493
- Williams A, Petriacq P, Schwarzenbacher R, Beerling D, Ton J (2018b) Mechanisms of glacial-to-future atmospheric CO<sub>2</sub> effects on plant immunity. *New Phytol* 218:752–761
- Yáñez-López R, Torres-Pacheco I, Guevara-González RG, Hernández-Zul MI, Quijano-Carranza JA, Rico-García E (2014) The effect of climate change on plant diseases. *Afr J Biotechnol* 11:2417–2428
- Yu X, Feng B, He P, Shan L (2017) From chaos to harmony: Responses and signaling upon microbial pattern recognition. *Annu Rev Phytopathol* 55:109–137
- Zavala JA, Nability PD, DeLucia EH (2013) An emerging understanding of mechanisms governing insect herbivory under elevated CO<sub>2</sub>. *Annu Rev Entomol* 58:79–97
- Zhang S, Li X, Sun Z, Shao S, Hu L, Ye M, Zhou Y, Xia X, Yu J, Shi K (2015) Antagonism between phytohormone signalling underlies the variation in disease susceptibility of tomato plants under elevated CO<sub>2</sub>. *J Exp Bot* 66:1951–1963
- Zhou Y, Vroegop-Vos I, Schuurink RC, Pieterse CMJ, Van Wees SCM (2017) Atmospheric CO<sub>2</sub> alters resistance of Arabidopsis to *Pseudomonas syringae* by affecting abscisic acid accumulation and stomatal responsiveness to coronatine. *Front Plant Sci* 8:700
- Zhou Y, Van Leeuwen SK, Pieterse CMJ, Bakker PAHM, Van Wees SCM (2019) Effect of atmospheric CO<sub>2</sub> on plant defense against leaf and root pathogens of Arabidopsis. *Eur J Plant Pathol* 154:31–42
- Zimmermann P, Hirsch-Hoffmann M, Hennig L, Gruissem W (2004) GENEVESTIGATOR. Arabidopsis microarray database and analysis toolbox. *Plant Physiol* 136:2621–2632
- Zipfel C, Robatzek S (2010) Pathogen-associated molecular pattern-triggered immunity: veni, vidi...? *Plant Physiol* 154:551–554

**Publisher's Note** Springer Nature remains neutral with regard to jurisdictional claims in published maps and institutional affiliations.